Investigating Molecular Charge Transfer Complexes
with a Low Temperature Scanning Tunneling Microscope

F. Jäckel,[1,2,†] U. G. E. Perera,[1] V. Iancu,[1] K.-F. Braun,[1] N. Koch,[2] J. P. Rabe,[2] and S.-W. Hla[1,*]

[1]*Ohio University, Physics & Astronomy Department, Athens, Ohio 45701, USA*
[2]*Humboldt-Universität zu Berlin, Institut für Physik, Newtonstraße 15, 12489 Berlin, Germany*

Electron donor-acceptor molecular charge transfer complexes (CTCs) formed by α-sexithiophene (6T) and tetrafluoro-tetracyano-quinodimethane (F_4TCNQ) on a Au(111) surface are investigated by scanning tunneling microscopy, spectroscopy, and spectroscopic imaging at 6 K. New hybrid molecular orbitals are formed in the CTCs, and the highest occupied molecular orbital of the CTC is mainly located on the electron accepting F_4TCNQ while the lowest unoccupied molecular orbital is predominantly positioned on the electron donating 6T. We observed the conductance switching of F_4TCNQ inside CTCs, which may find potential applications in novel molecular device operations.

Molecular charge transfer complexes (CTCs) [1,2] are an emerging class of materials having potential applications in molecular magnets [3–5], nonlinear optics [6,7], and molecular electronics [8–11]. CTCs are also used for doping organic materials as well as for energy storage applications [12–16]. Even though a number of organic CTCs have been studied for their structure and conductivity [17,18], investigations of CTC formation on the molecular level have yet to be reported. Such studies can provide new insight into the charge transfer mechanisms due to the absence of bulk effects [19,20] and ensemble averaging ubiquitous to conventional experimental techniques. Scanning tunneling microscopy (STM) and spectroscopy (STS) at low temperatures provide a unique tool to investigate properties of single molecules [21,22]. Here we present a low temperature STM and the first molecularly resolved STS study of organic CTCs formed by the electron donor α-sexithiophene (6T) and the electron acceptor tetrafluoro-tetracyano-quinodimethane (F_4TCNQ) on a Au(111) surface. We will show here that the CTC formation can be evidenced by bias dependent STM images, as well as by the dI/dV tunneling spectra and tunneling spectromicroscopy images.

The experiments were performed with a homebuilt ultrahigh vacuum STM operated at liquid helium temperatures [23]. The Au(111) sample was cleaned by cycles of Ne + -ion sputtering and annealing. The F_4TCNQ and 6T molecules (Sigma-Aldrich, 97% purity) were deposited on Au(111) between 50 K and 300 K substrate temperatures by thermal evaporation. The sample temperature was then reduced to 6 K for the experiment. Tunneling spectroscopy data and spectromicroscopy (dI/dV) images were directly acquired using a lock-in amplifier by adding 20 mV, 725 Hz ac modulation. An electrochemically etched tungsten wire was used as the STM tip, and the tip was further prepared *in situ* by dipping it into the Au(111) substrate [23]. The tip quality was checked by determining the well-

known Au(111) surface state [9] prior to each spectroscopic measurement [24].

The experimental procedure includes the following systematic steps: First, the electronic and structural properties of pure F_4TCNQ and 6T on Au(111) were separately determined by means of STM imaging and dI/dV spectroscopy. Next, F_4TCNQ-6T complexes were investigated by using STM imaging, dI/dV spectroscopy, and dI/dV mapping. The electronic structure changes due to the charge transfer process are then deduced by comparing the CTC data with that of the pure species.

F_4TCNQ [Fig. 1(a)] forms ordered self-assembled two-dimensional clusters [Figs. 1(b) and 1(c)] on Au(111) with unit cell lattice parameters of $a = (0.87 \pm 0.07)$ nm, $b = (1.22 \pm 0.08)$ nm, and $\alpha = (73 \pm 8)°$. The dI/dV spectra acquired over the centers of single molecules inside the cluster show states derived from the highest occupied molecular orbital (HOMO) and the HOMO-1 at −1 V and −1.4 V below the Fermi level, i.e., 0 V [Fig. 1(d)], and the lowest unoccupied molecular orbital (LUMO) at +0.6 V. In addition, shoulders at ca. −0.22 V and +0.22 V can be discerned, which are attributed to vibrational excitations [25].

In case of 6T on Au(111), the molecules adsorb in both straight and bent conformations (Fig. 2) [26]. The 6T molecules rarely form two-dimensional clusters on the Au(111) surface in low coverages. The dI/dV spectra measured on the center of 6T molecules show the HOMO and HOMO-1 levels at −0.8 V and −1.5 V, and the LUMO at +2 V, respectively, [Fig. 2(c)]. The splitting of the HOMO and HOMO-1 levels corresponds well to that obtained from photoemission for the weakly adsorbed 6T [27]. Both the straight and bent 6T conformations have similar HOMO and LUMO energy levels [28] and total energies [29].

Next, the 6T- F_4TCNQ molecular complexes are formed by depositing F_4TCNQ on 6T predeposited Au(111) or vice versa. Figure 3(a) presents a large area STM image
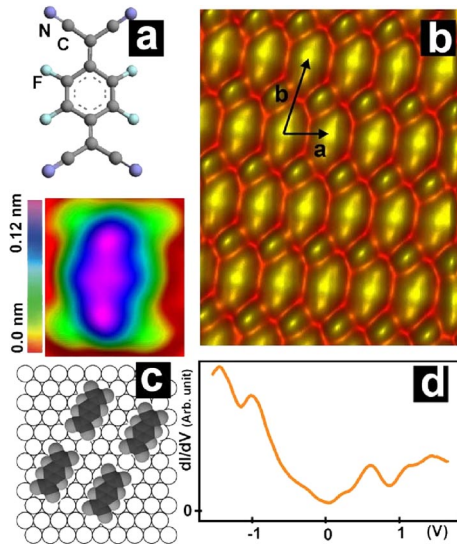
FIG. 1 (color online). Structure and electronic properties of the F$_4$TCNQ -Au(111) system at 6K. (a) A chemical model and an STM image of a single F$_4$TCNQ on Au(111). (Image parameters: 0.22 nA, −1.5 V.) (b) Self-assembled two-dimensional F$_4$TCNQ cluster on Au(111). (Image parameters: 0.35 nA, 0.8 V, 4 nm × 5.2 nm scan.) Note: The electron tunneling is from the HOMO-1 level to the tip in (a), and from the tip into a hybrid surface-LUMO state in (b). (c) Adsorption model of F$_4$TCNQ on Au(111). (d) dI/dV-V spectroscopy data of the F$_4$TCNQ-Au(111) system.

after deposition of F$_4$TCNQ on a 6T predeposited Au(111) surface at ∼120 K substrate temperature. Molecular clusters composed of 6T and F$_4$TCNQ can be found at both step edges and terraces, in a large manifold of relative mutual molecular conformations and orientations. Within clusters, 6T can adopt either straight or bent conformations [Figs. 3(a) and 3(b)] and the molecules do not form ordered structures. The exact orientations of the F$_4$TCNQ π systems inside the clusters cannot be known from the STM images; however, they are possibly noncoplanar with the substrate surface when the molecules are densely packed.

During STM imaging, some of the F$_4$TCNQs inside the molecular complexes can appear brighter when tunneling at a negative sample bias of ∼ − 1.5 V [30] [Fig. 3(b)]. An example is illustrated in Figs. 4(a) and 4(b) [28]. Figure 4(a) shows an STM image of a 6T-F$_4$TCNQ cluster acquired with a positive sample bias of +1.5 V. When the same cluster is imaged with −1.5 V [Fig. 4(b)], most of the F$_4$TCNQ locations certainly appear brighter, indicating that the F$_4$TCNQs inside the CTCs provide a higher tunneling current as compared to the neighboring 6T molecules at −1.5 V. This behavior is observed only in the densely packed clusters as shown in Fig. 4, where the two types of molecules appear in close contact with each other.

In order to gain insight into the charge transfer mechanism of 6T- F$_4$TCNQ complexes, dI/dV spectra of F$_4$TCNQ and 6T were measured on molecules inside the complexes. Since the two molecular species are positioned with different arrangements inside the clusters, several
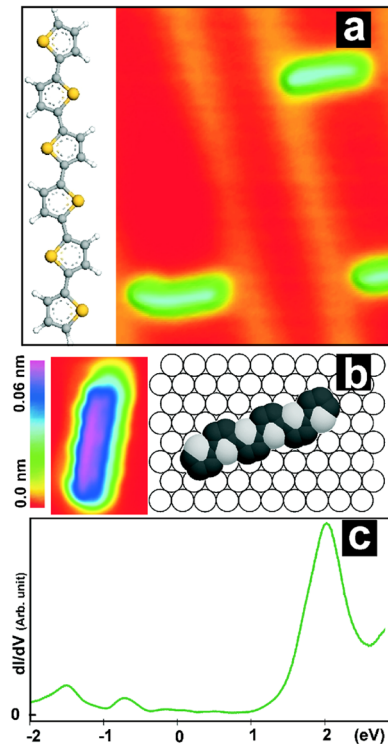

FIG. 2 (color online). Structure and electronic properties of the 6T-Au(111) system at 6 K. (a) STM image of isolated 6T molecules on Au(111) surface together with a chemical model [26]. (Image parameters are: 0.27 nA, −1.5 V, 7.5 nm × 9 nm scan.) (b) An adsorption model of 6T on Au(111) together with an STM image (1.7 nA, 0.2 V). (c) dI/dV spectroscopy data of the 6T-Au(111) system.

parameters, such as position, orientation, conformation, and distance between the molecules can influence the charge transfer process. Moreover, competing charge transfer processes might occur between F$_4$TCNQ chemisorbed on Au and F$_4$TCNQ in a CTC with 6T. Ultimately, we cannot exclude a ternary CTC formation involving Au, F$_4$TCNQ, and 6T. In this case, the charge transfer should involve the F$_4$TCNQ-Au(111) hybridized states. In order to get consistent results, an alternative approach was used: Only the centers of the bright spots are chosen as F$_4$TCNQ positions for the dI/dV measurements. For the 6T, the ones located next to the bright F$_4$TCNQ are selected. This selection provides a qualitative reproduction of dI/dV data for the two species inside the complex. The average dI/dV spectra of the 6T and F$_4$TCNQ inside the CTC are shown in Fig. 4(c) together with those dI/dV curves of pure F$_4$TCNQ and 6T for a comparison.

The dI/dV data of F$_4$TCNQ inside the CTCs give the HOMO and HOMO-1 levels at −1.2 V, and −1.6 V, and the LUMO level at +2 V [Fig. 4(c)], respectively. Here, both HOMO and HOMO-1 levels of F$_4$TCNQ in the complex are 0.2 eV shifted away from the Fermi level as compared to the pure F$_4$TCNQ [Fig. 4(c)]. In contrast to the pure F$_4$TCNQ on Au [Fig. 1(d)], we observe a clear-cut energy gap for F$_4$TCNQ in contact with 6T. In case of 6T
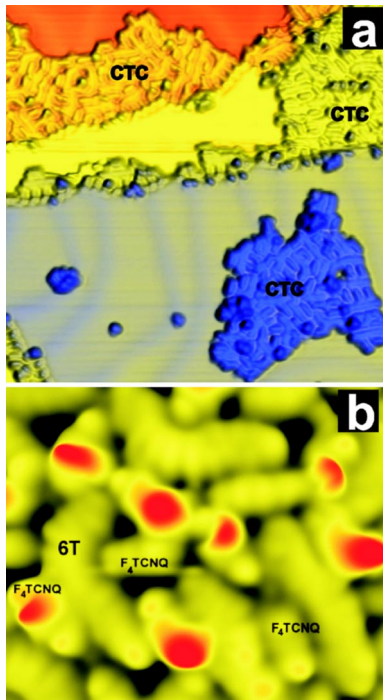
FIG. 3 (color online). 6T-F_4TCNQ mixed molecular clusters.
(a) STM image of the Au(111) surface showing molecular
clusters with mixed 6T and F_4TCNQ molecules (deposited at
~120 K) located at step edges and on terraces together with the
Au(111) surface herringbone reconstruction in the background.
(Image parameters: 0.1 nA, −1.5 V, 28 nm × 28 nm scan.)
(b) STM image of a mixed cluster illustrating a snapshot of
the mixed 6T and F_4TCNQ molecules [30]. The molecules are
positioned with a variety of orientations and conformations.
(Image parameters: 0.61 nA, −1.5 V, 6.5 nm × 5 nm scan.)

FIG. 4 (color online). Tunneling microscopy and spectroscopy
of 6T- F_4TCNQ charge transfer complexes. (a) STM image of a
6T- F_4TCNQ cluster with molecular complexes acquired at
+1.5 V, 0.43 nA. Here, both F_4TCNQ and 6T (shown with
white dots) appear with the same intensity. (b) When imaging
the same cluster at −1.56 V and 0.43 nA, the F_4TCNQ locations
appear brighter, while some F_4TCNQ remain at the same inten-
sity as before. (Image size: 9 nm × 10 nm.) (c) An averaged
dI/dV-V data set of F_4TCNQ and 6T inside the CTC generated
from 112 measurements; dashed curves are dI/dV-V data of
pure F_4TCNQ and 6T on Au(111). All the dI/dV-V curves are
vertically shifted to exhibit the same base level. The black
arrows indicate the shifting of level energies. The vertical dashed
lines are drawn for eye guidance. (d) A simultaneously recorded
STM image of CTCs together with a series of corresponding
dI/dV maps acquired at −1.7 V (e), −1.5 V (f), −1.0 V (g),
+0.8 V (h), and +1.5 V (i). The black and white arrows in the
dI/dV maps indicate the two classes of intensity variations at
F_4TCNQ locations. Notice the 6T locations are labeled in (d) and
(i).

inside the CTCs, the dI/dV data show the HOMO at
−1.6 V, and the LUMO and LUMO + 1 at +2 V, and
+2.5 V, respectively. Here, the 6T LUMO level in the
CTC is the same as the LUMO level of pure 6T, but the
LUMO level edge in the CTC is also shifted away from the
Fermi level [Fig. 4(c)] as compared to the pure 6T.
Moreover, the HOMO of 6T in the molecular complex
coincides with the HOMO-1 level of F_4TCNQ inside the
complex. The fact that the LUMO and HOMO level en-
ergies of F_4TCNQ and 6T within a CTC are virtually the
same indicates that the effective CTC-LUMO and CTC-
HOMO levels are delocalized over the complex. We sum-
marize our findings as follows: (1) Depopulation of the
neutral 6T HOMO, and a lowering of F_4TCNQ occupied
orbital energies occur in the CTC as compared to the corre-
sponding neutral molecules. (2) The F_4TCNQ LUMO is
realigned to the 6T LUMO level in the complex. (3) The
hybrid CTC-HOMO is mainly located on the electron
acceptor F_4TCNQ while the CTC-LUMO is predominantly
positioned on the electron donor 6T, with some contribu-
tion on F_4TCNQ.

These findings lead us to conclude that, indeed, 6T-
F_4TCNQ charge transfer complexes are formed on the
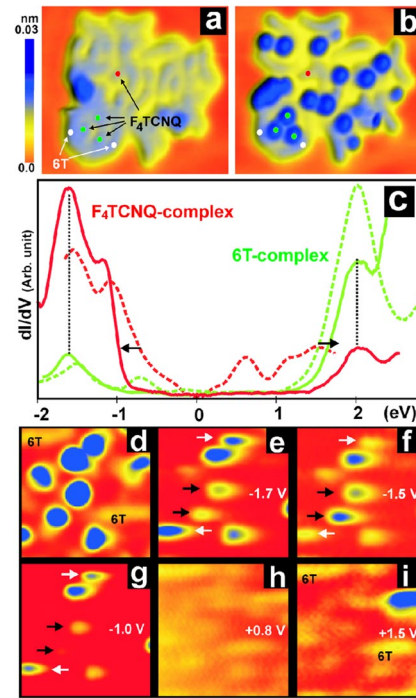Au(111) surface, however, with a manifold of different

conformations. The charge transfer between the two mole-
cules results in a lowering of the HOMO level in the
electron acceptor F_4TCNQ, and thus, the molecule be-
comes negatively charged. In case of the electron donor
6T, the LUMO edge energy increases, and therefore, the 6T
becomes positively charged. We can now explain the
higher current intensity of F_4TCNQ in the complex when
tunneling at negative biases as being due to the formation
of new HOMO levels, originating from the charge transfer
process. STM imaging using biases matching these orbital
energies can thus provide resonance tunneling. The highest
intensities of the bright areas are mostly located at the
centers of the F_4TCNQ in the complex [Fig. 3(b)]. This
suggests that the transfer charge strongly involves the
central π system of the molecule.

In order to further confirm and visualize the charge transfer mechanism, the spectroscopic images (dI/dV maps) of CTCs are acquired and presented in Figs. 4(e)–4(i). Figure 4(d) illustrates a STM image simultaneously recorded with -1.5 V during the spectroscopic imaging where the bright (blue) areas provide F_4TCNQ locations as in Fig. 4(b). The dI/dV maps acquired at -1.7 V [Fig. 4(e)], -1.5 V [Fig. 4(f)], and -1 V [Fig. 4(g)] reveal the intensity changes of F_4TCNQ locations based on the specific bias. For instance, the areas indicated with the white arrows provide higher intensities at -1.7 V and -1 V but a reduced intensity at -1.5 V. This is in accordance with the HOMO-1 and HOMO levels of F_4TCNQ inside the CTCs [Fig. 4(c)]. The areas shown with black arrows have the highest intensities at -1.5 V, but their intensities are reduced at -1.7 V and -1 V. The changes in dI/dV intensities might be originated by the variations in orbital energies based on the different molecular conformations and packing. At $+0.8$ V bias no apparent features appear in the dI/dV map [Fig. 4(h)] because this energy is within the CTC energy gap. At $+1.5$ V, faint features appear at both F_4TCNQ and 6T locations with 6Ts providing slightly higher intensities. This can be explained by $+1.5$ V being located at the upward slope of the CTC-LUMO [Fig. 4(c)], and the dI/dV curve shows higher intensity for the 6T LUMO as compared to that of F_4TCNQ. Thus, these spectromicroscopy images confirm the individual dI/dV spectra of CTCs shown in Fig. 4(c). Since the curve in Fig. 4(c) is an averaged data presentation, the slight variations in orbital energies of specific CTC units can now be visualized in detail.

In summary, we report the tunneling microscopy, spectroscopy, and spectromicroscopy studies of the molecular charge transfer inside an electron donor-acceptor molecular complex, 6T-F_4TCNQ. We also show that the intermolecular charge transfer can lead to realignment of molecular orbitals and to the formation of new hybrid HOMO and LUMO levels for the complex. Moreover, our resonance tunneling scheme allows observing conductance switching of one type of molecule inside the complex, which is not only useful to distinguish between the charge transfer species but also may find potential applications in novel molecular device operations.

---

*Corresponding author.
hla@ohio.edu
www.phy.ohiou.edu/~hla

†Stanford University, Department of Chemistry, 333 Campus Drive, Stanford, CA 94305, USA.
[1] R. S. Mulliken, J. Am. Chem. Soc. **72**, 600 (1950).
[2] *Handbook of Organic Conductive Molecules and Polymers*, edited by H. S. Nalwa (John Wiley & Sons, Chichester, 1997).
[3] P. M. Allemand et al., Science **253**, 301 (1991).
[4] B. Narymbetov et al., Nature (London) **407**, 883 (2000).
[5] S. J. Blundell and F. L. Pratt, J. Phys. Condens. Matter **16**, R771 (2004).
[6] H. S. Nalwa, Adv. Mater. **5**, 341 (1993).
[7] A. Krishnan, S. K. Pal, P. Nandakumar, A. G. Samuelson, and P. K. Das, Chem. Phys. **265**, 313 (2001).
[8] F. Jäckel, M. D. Watson, K. Müllen, and J. P. Rabe, Phys. Rev. Lett. **92**, 188303 (2004).
[9] N. Koch, S. Duhm, J. P. Rabe, A. Vollmer, and R. L. Johnson, Phys. Rev. Lett. **95**, 237601 (2005).
[10] P. Samori, N. Severin, C. D. Simpson, K. Müllen, and J. P. Rabe, J. Am. Chem. Soc. **124**, 9454 (2002).
[11] J. R. Gong et al., J. Phys. Chem. B **109**, 1675 (2005).
[12] M. Keil et al., Chem. Phys. **116**, 10854 (2002).
[13] N. Koch et al., J. Phys. Chem. B **104**, 1434 (2000).
[14] W. Y. Gao and A. Kahn, Appl. Phys. Lett. **79**, 4040 (2001).
[15] J. G. Xue and S. R. Forrest, Phys. Rev. B **69**, 245322 (2004).
[16] J. Blochwitz, M. Pfeiffer, T. Fritz, and K. Leo, Appl. Phys. Lett. **73**, 729 (1998).
[17] S. Hotta and H. Kobayashi, Synth. Met. **66**, 117 (1994).
[18] G. Brocks, Phys. Rev. B **55**, 6816 (1997).
[19] F. Zwick et al., Phys. Rev. Lett. **81**, 2974 (1998).
[20] T. Nishiguchi, M. Kageshima, N. Ara-Kato, and A. Kawazu, Phys. Rev. Lett. **81**, 3187 (1998).
[21] V. Iancu, A. Deshpande, and S.-W. Hla, Phys. Rev. Lett. **97**, 266603 (2006).
[22] K.-F. Braun, V. Iancu, N. Pertalya, K.-H. Rieder, and S.-W. Hla, Phys. Rev. Lett. **96**, 246102 (2006).
[23] S.-W. Hla, J. Vac. Sci. Technol. B **23**, 1351 (2005).
[24] The tip is held at ground and all the biases referred to in the text are the sample voltages. The tunneling spectroscopy data are averaged over hundreds of different molecules from eight separate experimental runs.
[25] B. C. Stipe, M. Rezaei, and W. Ho, Science **280**, 1732 (1998).
[26] We observe a variety of 6T bent conformations with varying angles. The C–C bond rotation of the molecule could cause the bent conformations, which might be induced during the thermal evaporation.
[27] N. Koch et al., Chem. Phys. Lett. **413**, 390 (2005).
[28] See EPAPS Document No. E-PRLTAO-100-075809 for tunneling spectroscopy data of bent and straight 6T on Au(111), and the CTCs formed by depositing 6T on a F_4TCNQ -Au(111) system. For more information on EPAPS, see http://www.aip.org/pubservs/epaps.html.
[29] H. Glowatzki, S. Duhm, K.-F. Braun, J. P. Rabe, and N. Koch, Phys. Rev. B **76**, 125425 (2007).
[30] When the 6T-F_4TCNQ complexes are formed above 50 K substrate temperature, some of the complexes are loosely packed and may not show the brighter appearance as in Fig. 4. The charge transfer effect is observed in all the 6T-F_4TCNQ complexes deposited at $\sim$50 K substrate temperature where the molecules are densely packed.